Electric detection of spin wave resonance using inverse spin-Hall effect

doi: 10.1063/1.3167826

Electric detection of spin wave resonance using inverse spin-Hall effect

K. Ando,[1,2,a] J. Ieda,[2,3] K. Sasage,[2] S. Takahashi,[2,3] S. Maekawa,[2,3] and E. Saitoh[1,2,4]
[1]*Department of Applied Physics and Physico-Informatics, Keio University, Yokohama 223-8522, Japan*
[2]*Institute for Materials Research, Tohoku University, Sendai 980-8577, Japan*
[3]*CREST, Japan Science and Technology Agency, Sanbancho, Tokyo 102-0075, Japan*
[4]*PRESTO, Japan Science and Technology Agency, Sanbancho, Tokyo 102-0075, Japan*

(Received 1 June 2009; accepted 11 June 2009; published online 1 July 2009)

Spin wave resonance in $Ni_{81}Fe_{19}$/Pt thin wire arrays has been investigated using the inverse spin-Hall effect (ISHE). The spin wave in the $Ni_{81}Fe_{19}$ layer drives spin pumping, generation of spin currents from magnetization precession, and the pumped spin current is converted into a charge current by ISHE in the Pt layer. We found an electromotive force transverse to the spatial and the spin-polarization directions of the spin current. The experimental results indicate that the amplitude of the electromotive force is proportional to the spin wave resonance absorption intensity, enabling the electric measurement of spin wave resonance in nanostructured magnetic systems. © *2009 American Institute of Physics*. [DOI: 10.1063/1.3167826]

There is currently great interest in the field of spintronics, which is a new device technology promising efficient magnetic memories and computing devices based on electron spins.[1,2] The field of spintronics aims to extend the scope of conventional electronics by controlling magnetization dynamics using a spin current, a flow of electron spins in a solid.[3] In this stream, intensive experimental interests have been focused on a method for electric detection of magnetic resonance,[4,5] which enables the electric investigation of magnetization dynamics in magnetic systems.

The electric detection of ferromagnetic resonance can be achieved using the spin pumping[6–8] and the inverse spin-Hall effect (ISHE)[9–17] in ferromagnetic/paramagnetic bilayer systems.[9] The electromotive force due to ISHE induced by the spin pumping was recently observed in $Ni_{81}Fe_{19}$/Pt bilayer films.[9,13,18] Up to now, studies on the spin pumping have been mainly focused on the uniform magnetization precession in thin film systems. However, spintronic devices operate in micro- or nanoscale systems. By reducing the system size, the magnetization dynamics changes dramatically; in confined magnetic systems, the dynamics is governed by spin wave modes, a situation in contrast to the almost uniform precession of magnetization in extended thin films. The electric detection of spin wave resonance using the spin wave spin pumping (SWSP) is yet to be established.

In this letter, we demonstrate the electric detection of spin wave resonance in $Ni_{81}Fe_{19}$/Pt thin wire arrays using ISHE induced by SWSP. This method allows the electric and direct detection of spin wave resonance without using oscillating electric currents, and thus will be useful for developing spintronic devices as well as for investigating spin dynamics in nanostructured systems.

Figures 1(a) and 1(b) show a schematic illustration and a scanning electron microscope (SEM) image of the sample used in the present study. The samples are an array of $Ni_{81}Fe_{19}$/Pt thin wires with width $w=1$, 1.5, and 2 μm comprising a 10-nm-thick Pt layer and a 30-nm-thick $Ni_{81}Fe_{19}$ layer. The wires were arranged with the 1 μm spacing over a range of 500 μm. The thin wires were fabricated using the electron beam lithography and the lift-off technique. The Pt layer was first deposited on a thermally oxidized Si substrate by sputtering, and then the $Ni_{81}Fe_{19}$ layer was evaporated in a high vacuum. Each wire is connected by a 5-nm-thick AuPd electrode layer, which is sputtered on the whole substrate. Two electrodes are attached to both ends of the AuPd layer.

For the measurement, the sample system is placed near the center of a TE_{011} cavity at which the magnetic-field component of the microwave mode is maximized while the electric-field component is minimized. During the measurement, the microwave mode with frequency $f=9.441$ GHz exists in the cavity, and an external magnetic field **H** is applied along the wires as illustrated in Fig. 1(b). When H and f fulfill the resonance condition, a spin current is resonantly injected into the Pt layer by the spin pumping. This injected spin current is converted into a charge current by ISHE in the Pt layer and causes an electric potential difference between the edges of the Pt layer. The electric potential difference is

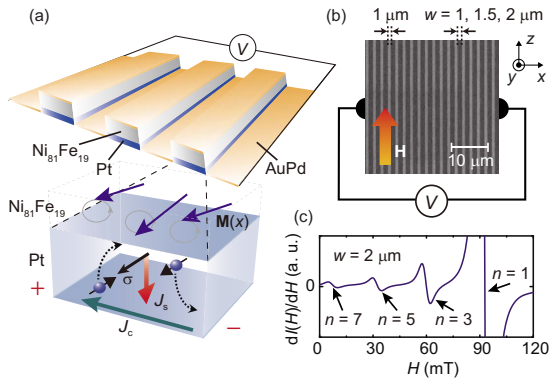

FIG. 1. (Color online) (a) A schematic illustration of the spin pumping and the inverse spin-Hall effect in the $Ni_{81}Fe_{19}$/Pt thin wires. J_c, J_s, and σ represent a charge current, a spin current, and the spin polarization of the spin current, respectively. $\mathbf{M}(x)$ denotes the magnetization. (b) A SEM image of the $Ni_{81}Fe_{19}$/Pt thin wires consisted of a periodic array of $w=1$ μm thin wires. w shows the wire width. **H** is the external magnetic field. (c) Field (H) dependence of the FMR signal $dI(H)/dH$ for the $w=2$ μm $Ni_{81}Fe_{19}$/Pt wires. Here, I denotes the microwave absorption intensity.

[a]Electronic addresses: kazuya_ando@z8.keio.jp.

summed over the array along the x direction, giving rise to an amplified electromotive force signal between the edges of the sample. Using the field-lock-in technique, we measured simultaneously the microwave absorption signal and the electromotive force V between the electrodes attached to the AuPd layer. The magnetodipole interaction between the wires is negligibly small for the 1 μm separation.[19,20] All the measurements were performed at room temperature.

Figure 1(c) shows the microwave absorption spectrum in the $Ni_{81}Fe_{19}$/Pt thin wires ($w=2$ μm) under the 200 mW microwave excitation with the external magnetic field along the wire axis. In contrast to a single FMR peak observed in $Ni_{81}Fe_{19}$ films corresponding to the uniform magnetization precession,[9] multiple resonance signals appear in the wires. These multiple signals are observed also in the wires of $w=1$ and 1.5 μm [see Figs. 2(a) and 2(e)]. The observed multiple resonance fields are consistent with a model of the spin wave resonance for the effective dipolar boundary conditions,[21] in which the effective pinning is determined by the inhomogeneity of the dynamical demagnetization field near the edges of the wire. In this model, the symmetric components of the eigenfunctions across the width of the wire have the form

$$m_n(x) = A_n \cos(\kappa_n x) \ (n = 1,3,5,7,\ldots), \tag{1}$$

as shown in Fig. 3(b). x is the coordinate along the wire width direction [see Fig. 1(b)]. Here, κ_n is the quantized wave number: $\kappa_n = n\pi[1-2/d(p)]/w$, where $d(p)=2\pi/\{p[1+2\ln(1/p)]\}$ is the dimensionless effective pinning parameter and $p=t/w$ is the aspect ratio of the wire (t is the thickness of the $Ni_{81}Fe_{19}$ layer). Only the symmetric modes, which have nonzero average dipolar moments, can be excited by a uniform microwave. The resonance field of the nth mode in this model is approximately expressed as

$$H_n = 4\pi M_s \left[\frac{1}{2}(\sqrt{1+4\tilde{\omega}^2}-1) - \frac{\pi(2n-1)}{4\sqrt{1+4\tilde{\omega}^2}} \frac{t}{w} \right], \tag{2}$$

where $\tilde{\omega} \equiv (\omega/\gamma)/(4\pi M_s)$. Equation (2) shows that the resonance field H_n is linearly dependent on the mode number n and the mode separation $\Delta H \equiv H_n - H_{n+2}$ is inversely proportional to the wire width w as

$$\Delta H = \frac{(4\pi M_s)t\pi}{\sqrt{1+4\tilde{\omega}^2}} \frac{1}{w}. \tag{3}$$

These features are consistent with the experimental results as shown in Fig. 3(a); the experimental results are well reproduced by Eq. (3) using the parameters $\omega = 5.93\times10^{10}$ s^{-1}, $\gamma = 1.86\times10^{11}$ T^{-1} s^{-1}, $4\pi M_s = 0.795$ T, and $t=30$ nm.

In Figs. 2(b), 2(f), and 2(j), we show the field dependence of $dV(H)/dH$ for the $w=1$, 1.5, and 2 μm $Ni_{81}Fe_{19}$/Pt wire arrays, respectively. The resonant electromotive force signals appear for all the samples. The field positions of these signals coincide with the microwave spin wave-resonance fields; the electromotive force follows the same selection rule as the spin wave microwave absorption.

In order to elucidate the origin of the electromotive force observed in the $Ni_{81}Fe_{19}$/Pt wires, we measured $dV(H)/dH$ for a $Ni_{81}Fe_{19}$ wire array ($w=2$ μm), in which the Pt layer is missing. The $Ni_{81}Fe_{19}$ wire shows no electromotive force signal as shown in the inset to Fig. 2(j), demonstrating that the electromotive force observed in the $Ni_{81}Fe_{19}$/Pt wires is

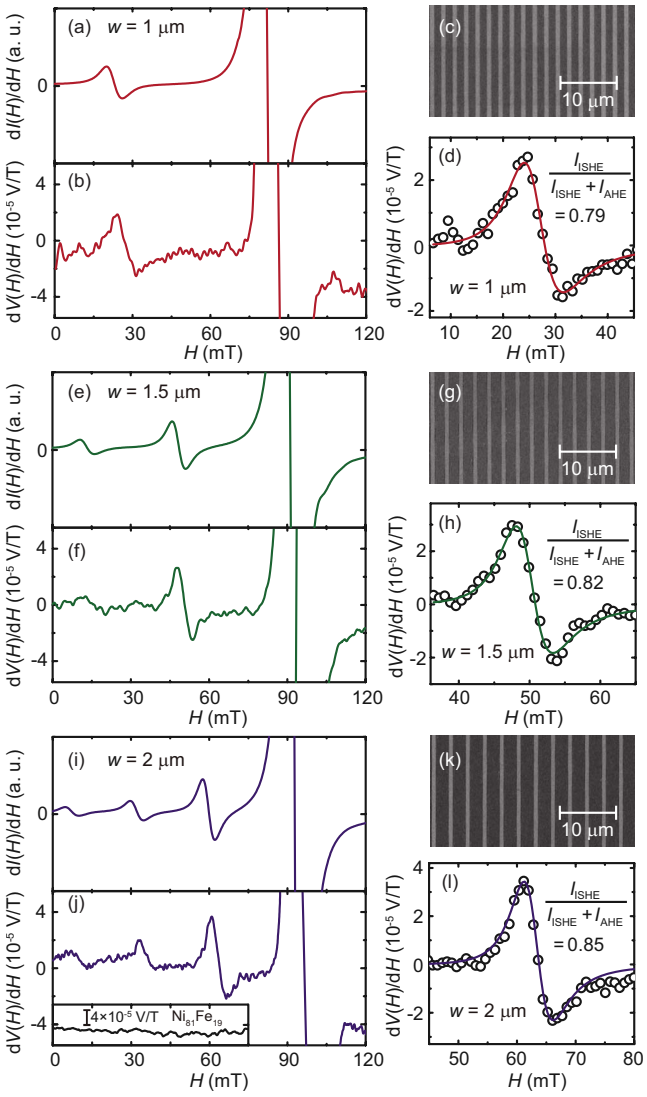

FIG. 2. (Color online) [(a), (e), and (i)] Field (H) dependence of the FMR signal $dI(H)/dH$ in the $Ni_{81}Fe_{19}$/Pt wire arrays with $w=1$, 1.5, and 2 μm, respectively. Here, I denotes the microwave absorption intensity. [(b), (f), and (j)] $dV(H)/dH$ in the $Ni_{81}Fe_{19}$/Pt wire arrays with $w=1$, 1.5, and 2 μm, respectively. V denotes the electric-potential difference between the electrodes attached to the AuPd layer. The inset to (j) shows $dV(H)/dH$ in the $Ni_{81}Fe_{19}$ wire array ($w=2$ μm). [(c), (g), and (k)] SEM images of the $w=1$, 1.5, and 2 μm $Ni_{81}Fe_{19}$/Pt wire arrays, respectively. [(d), (h), and (l)] The $dV(H)/dH$ observed for the $n=3$ mode spin wave resonance for the $Ni_{81}Fe_{19}$/Pt wire arrays with $w=1$, 1.5, and 2 μm, respectively. The solid curves are the fitting results using the dispersion function I_{ISHE} and the double-bump function I_{AHE} (Ref. 9).

due not to the extrinsic magnetogalavanic effects, e.g., the anomalous Hall effect,[18] but is due to ISHE induced by SWSP. This is supported also by the spectral shape analysis for the electromotive force. The observed almost symmetric dispersion shape of the electromotive force spectra [Figs. 2(d), 2(h), and 2(l)] is consistent with the prediction of the spin-pumping-induced ISHE.[9,18]

In Figs. 4(b)–4(d), the amplitude of the ISHE signal V'_n is plotted as a function of the microwave power P_{MW}, where V'_n is estimated as the total amplitude of $dV(H)/dH$ [see Fig. 4(a)]. The amplitude increases linearly with the microwave power, supporting the SWSP scenario as follows. In the standard model of the spin pumping,[6] the generated spin current density $\mathbf{j}_s \propto (\mathbf{M} \times d\mathbf{M}/dt)$, where $\mathbf{M}$ is the magnetization. In the present system, the dc component $j_s(x)$ is the time aver-

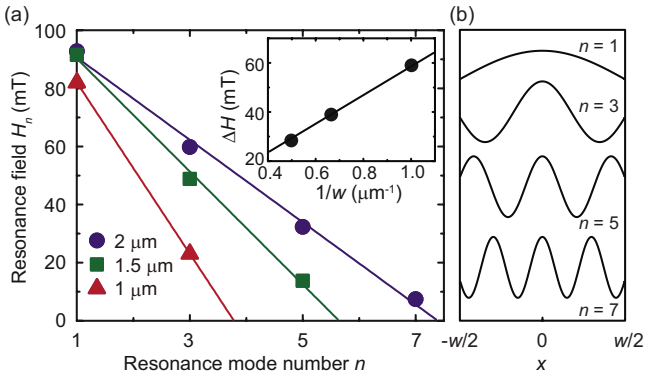

FIG. 3. (Color online) (a) The spin wave resonance field H_n as a function of the mode number n for the $Ni_{81}Fe_{19}$/Pt wires of the width w=1, 1.5, and 2 μm. The solid lines show linear fits to the data. The inset shows the mode separation $\Delta H \equiv H_n - H_{n+2}$ plotted as a function of $1/w$. The solid line shows a fitting result using Eq. (3). The resonance field is insensitive to surface roughness compared to the spectral amplitude (Ref. 23). (b) The spin wave eigenmode profiles along the wire width direction x.

aged z component of $\mathbf{j}_s(x)$: $j_s(x) \propto (\omega/2\pi)\int_0^{(2\pi/\omega)}[\mathbf{M}(x) \times d\mathbf{M}(x)/dt]_z dt$, where $\omega = 2\pi f$ and f is the microwave frequency. The pumped spin current does not depend on the phase of the spin wave modes, since only the z component has nonzero time average. The total spin current can be obtained as $J_s = \int j_s(x)dx \propto \omega\chi'' h^2$ in the same manner as in the case of thin film systems.[13,18] Here, χ'' is the imaginary part of the transverse magnetic susceptibility and h is the amplitude of the microwave magnetic field. In the spin wave resonance $\chi'' = \Sigma_n \chi_n''$ where $\chi_n'' \propto |\int m_n(x)dx|^2 / \int |m_n(x)|^2 dx$ for the nth mode spin wave.[22] Therefore, the spin current injected into the Pt layer due to the nth mode resonance is

$$J_s^n \propto \omega \chi_n'' h^2. \tag{4}$$

Equation (4) shows that the induced spin current J_s^n is proportional to h^2, which is consistent with the measured P_{MW} dependence of V_n' shown in Fig. 4. Equation (4) also shows

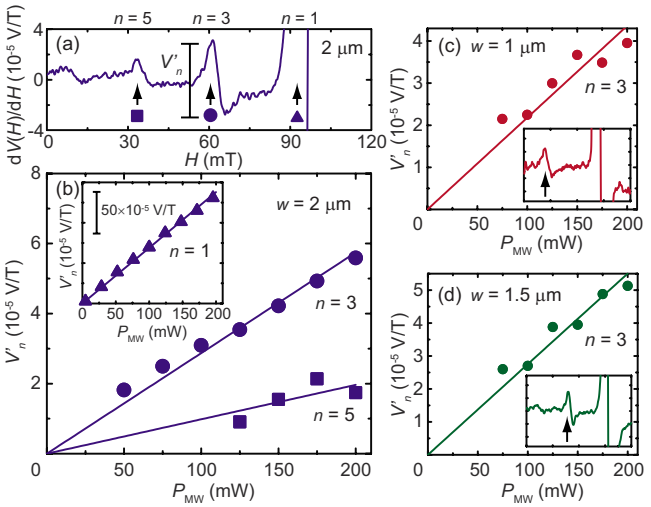

FIG. 4. (Color online) (a) $dV(H)/dH$ signal for the w=2 μm $Ni_{81}Fe_{19}$/Pt thin wire array. n is the mode number. V_n' shows the amplitude of the ISHE signal. (b) Microwave power P_{MW} dependence of the ISHE signal V_n' for the 2 μm $Ni_{81}Fe_{19}$/Pt thin wire array. Here, V_n' is estimated as the total amplitude of $dV(H)/dH$ for the nth mode spin wave resonance [see (a)]. [(c) and (d)] The P_{MW} dependence of V_n' for the w=1 and 1.5 μm $Ni_{81}Fe_{19}$/Pt thin wires, respectively. In the insets, the data in Figs. 2(b) and 2(f) are replotted for comparison.

TABLE I. Comparison of the normalized microwave absorption intensity $I_n'/I_{n=1}'$ and the normalized amplitude of the ISHE signal $V_n'/V_{n=1}'$ for the 2 μm $Ni_{81}Fe_{19}$/Pt thin wire array. I_n' and V_n' are defined as the total amplitude of the resonance shape [see Fig. 4(a)].

n	1	3	5	7
$I_n'/I_{n=1}'$	1.00	0.0414	0.0144	0.00743
$V_n'/V_{n=1}'$	1.00	0.0415	0.0129	0.00786

that J_s^n is proportional to the microwave absorption intensity $I_n = (\omega h^2/2)\chi_n''$, indicating that the spectral shape and the relative intensity of the electromotive force due to ISHE induced by SWSP are expected to be identical to those of the microwave absorption. These are demonstrated in the present experiments, as shown in Fig. 2 and Table I.

In summary, we demonstrated the electric detection of spin wave resonance in $Ni_{81}Fe_{19}$/Pt thin wire arrays using the SWSP and the ISHE. This method allows the electric investigation of spin dynamics in confined nanoscale systems.

This work was supported by a Grant-in-Aid for Scientific research in Priority Area "Creation and control of spin current," Scientific Research A, Nanoscience Program of Next Generation Supercomputing Project, and by Global COE Program "High-Level Global Cooperation for Leading-Edge Platform on Access Spaces (C12)" from MEXT.

[1] I. Zutic, J. Fabian, and S. D. Sarma, Rev. Mod. Phys. **76**, 323 (2004).
[2] *Concepts in Spin Electronics*, edited by S. Maekawa (Oxford University Press, Oxford, 2006).
[3] K. Ando, S. Takahashi, K. Harii, K. Sasage, J. Ieda, S. Maekawa, and E. Saitoh, Phys. Rev. Lett. **101**, 036601 (2008).
[4] X. Hui, A. Wirthmann, Y. S. Gui, Y. Tian, X. F. Jin, Z. H. Chen, S. C. Shen, and C.-M. Hu, Appl. Phys. Lett. **93**, 232502 (2008).
[5] Y. S. Gui, N. Mecking, A. Wirthmann, L. H. Bai, and C.-M. Hu, Appl. Phys. Lett. **91**, 082503 (2007).
[6] Y. Tserkovnyak, A. Brataas, and G. E. W. Bauer, Phys. Rev. Lett. **88**, 117601 (2002).
[7] S. Mizukami, Y. Ando, and T. Miyazaki, Phys. Rev. B **66**, 104413 (2002).
[8] M. V. Costache, M. Sladkov, S. M. Watts, C. H. van der Wal, and B. J. van Wees, Phys. Rev. Lett. **97**, 216603 (2006).
[9] E. Saitoh, M. Ueda, H. Miyajima, and G. Tatara, Appl. Phys. Lett. **88**, 182509 (2006).
[10] T. Kimura, Y. Otani, T. Sato, S. Takahashi, and S. Maekawa, Phys. Rev. Lett. **98**, 156601 (2007).
[11] S. O. Valenzuela and M. Tinkham, Nature (London) **442**, 176 (2006).
[12] S. Takahashi and S. Maekawa, Phys. Rev. Lett. **88**, 116601 (2002).
[13] K. Ando, Y. Kajiwara, S. Takahashi, S. Maekawa, K. Takemoto, M. Takatsu, and E. Saitoh, Phys. Rev. B **78**, 014413 (2008).
[14] K. Ando, T. Yoshino, and E. Saitoh, Appl. Phys. Lett. **94**, 152509 (2009).
[15] A. Takeuchi and G. Tatara, J. Phys. Soc. Jpn. **77**, 074701 (2008).
[16] K. Harii, K. Ando, H. Y. Inoue, K. Sasage, and E. Saitoh, J. Appl. Phys. **103**, 07F311 (2008).
[17] K. Uchida, S. Takahashi, K. Harii, J. Ieda, W. Koshibae, K. Ando, S. Maekawa, and E. Saitoh, Nature (London) **455**, 778 (2008).
[18] H. Y. Inoue, K. Harii, K. Ando, K. Sasage, and E. Saitoh, J. Appl. Phys. **102**, 083915 (2007).
[19] C. Mathieu, J. Jorzick, A. Frank, S. O. Demokritov, A. N. Slavin, B. Hillebrands, B. Bartenlian, C. Chappert, D. Decanini, F. Rousseaux, and E. Cambril, Phys. Rev. Lett. **81**, 3968 (1998).
[20] J. Jorzick, S. O. Demokritov, C. Mathieu, B. Hillebrands, B. Bartenlian, C. Chappert, F. Rousseaux, and A. N. Slavin, Phys. Rev. B **60**, 15194 (1999).
[21] K. Y. Guslienko, S. O. Demokritov, B. Hillebrands, and A. N. Slavin, Phys. Rev. B **66**, 132402 (2002).
[22] C. Bihler, W. Schoch, W. Limmer, S. T. B. Goennenwein, and M. S. Brandt, Phys. Rev. B **79**, 045205 (2009).
[23] K. Ando, K. Sasage, K. Harii, and E. Saitoh, Phys. Status Solidi B **244**, 4522 (2007).